NANO LETTERS

2007
Vol. 7, No. 6
1817−1822

The Morphology of Axial and Branched Nanowire Heterostructures

Kimberly A. Dick,*,† Suneel Kodambaka,‡ Mark C. Reuter,‡ Knut Deppert,† Lars Samuelson,† Werner Seifert,† L. Reine Wallenberg,§ and Frances M. Ross‡,§

Solid State Physics, Lund University, Box 118, S-221 00 Lund, Sweden, IBM Research Division, T. J. Watson Research Center, Yorktown Heights, New York 10598, Polymer and Materials Chemistry/nCHREM, Lund University, Box 124, S-221 00 Lund, Sweden

Received March 13, 2007; Revised Manuscript Received April 20, 2007

ABSTRACT

We present an extensive investigation of the epitaxial growth of Au-assisted axial heterostructure nanowires composed of group IV and III–V materials and derive a model to explain the overall morphology of such wires. By analogy with 2D epitaxial growth, this model relates the wire morphology (i.e., whether it is kinked or straight) to the relationship of the interface energies between the two materials and the particle. This model suggests that, for any pair of materials, it should be easier to form a straight wire with one interface direction than the other, and we demonstrate this for the material combinations presented here. However, such factors as kinetics and the use of surfactants may permit the growth of straight double heterostructure nanowires. Finally, we demonstrate that branched nanowire heterostructures, also known as nanotrees, can be successfully explained by the same model.

Nanowires offer great advantage in the fabrication of heterostructure devices because their narrow diameter allows for efficient strain relaxation and the formation of epitaxial structures from lattice-mismatched materials.[1,2] Nanowires whose composition varies along their length (axial heterostructure nanowires) composed of Si−Ge,[3] InAs−InP,[4] and GaAs−GaP[5,6] have already been demonstrated with sharp interfaces in both interface directions; all of these systems have lattice mismatches greater than 3%. The growth of such wires, where the interface quality is good in both directions and the wire is straight, is necessary to form structures containing thin barriers and quantum dots. Demonstrations of nanowire heterostructures containing ternary III−V materials, such as GaAsP,[7] InAsP,[8] or InGaAs,[9] further increase the potential for heterostructure applications. The development of other material combinations, using both III−V and IV materials, is of great interest in order to expand the range of device possibilities. However, it is not clear a priori whether it is possible to make arbitrary materials combinations into nanowires with good morphology. We have therefore investigated a variety of group IV and III−V material combinations in order to develop an understanding of the factors that affect the morphology of axial heterostructure nanowires as well as the morphology of branched nanowire structures.

Heterostructure nanowires were grown by low-pressure metal organic vapor-phase epitaxy (LP-MOVPE, 7.5 Torr in 6 L/min H_2) by combining the III−V materials GaAs, GaP, InAs, InP, and AlAs as well as Si. Growth was performed using size-selected Au aerosol particles[10] with a diameter of 40 nm and surface density of 0.5 μm^{-2}. The precursor materials arsine (AsH_3), phosphine (PH_3), trimethylgallium (TMG), trimethylindium (TMI), trimethylaluminum (TMA), and disilane (Si_2H_6) were used. Growth conditions were chosen within the established temperature and precursor pressure ranges for each material.[11−15] For AlAs and Si (the growth of which has not previously been reported for our system), the temperature ranges used were 420−480 °C and 625−650 °C, respectively. Samples were grown on III−V (111)B or Si(111) substrates appropriate to the desired growth. GaP and GaAs substrates were annealed before growth (to 650 °C in H_2/PH_3 or H_2/AsH_3) to desorb surface oxides; other substrates were heated directly to the growth temperature. No annealing was performed between heterostructure segments. Sharp heterostructure interfaces were obtained by flushing with hydrogen (at growth temperature) for several minutes between growths of the two different semiconductor materials to remove residual precursor material. When different growth temperatures were desired, the temperature was also ramped during this step. Note that the analysis presented below does not apply to "diffuse" interfaces, where the wire composition changes gradually between the two materials.

The combinations InAs−InP, GaAs−GaP, GaAs−InP, InAs−InP, InAs−GaP, InAs−AlAs, and GaAs−InP were investigated throughout the appropriate parameter ranges in both interface directions to determine any dependence of

* Corresponding author. E-mail: Kimberly.dick@ftf.lth.se.
† Solid State Physics, Lund University.
‡ IBM Research Division, T. J. Watson Research Center.
§ Polymer & Materials Chemistry/nCHREM, Lund University.

10.1021/nl0705900 CCC: $37.00
Published on Web 05/10/2007

morphology on growth conditions. The combinations GaAs−AlAs, GaP−AlAs, InP−AlAs, GaP−Si, and GaAs−Si were investigated at several selected conditions within the appropriate range.

Additionally, the combinations GaP−Ge and GaP−Si were grown by ultrahigh vacuum chemical vapor deposition (UHV-CVD). This growth was carried out in an in situ transmission electron microscope (a Hitachi H-9000 TEM with base pressure 2×10^{-10} Torr operated at 300 kV) so that the growth process could be examined in real time.[16] Slices of Si substrate on which GaP wires had been grown (by MOVPE, as above) were fitted directly into the TEM holder so that the wires intended for investigation were perpendicular to the electron beam. After heating to a suitable temperature (between 400 and 600 °C for Si and between 300 and 400 °C for Ge), the samples were exposed to disilane or digermane (Ge_2H_6) with a pressure around 1×10^{-5} Torr.[17,18]

Finally, branched heterostructures were also grown by depositing a second set of Au aerosol particles onto first-generation nanowires and performing a second growth step. Branches were grown by both MOVPE and UHV-CVD, using a selection of the materials and parameters described above.

During these experiments, we observe that the growth behavior typically falls into one of two categories. In some systems, the nanowire growth continues in the same crystal direction when the second material is introduced ("straight nanowires"); this is the case for example when growing InP → GaP or Si → GaP (Figure 1a,b). Here the notation A → B refers to the epitaxial growth of material B on material A, while the notation A−B refs to the combination of A and B, without reference to interface direction. In other cases, however, the wires tend to kink, or wrap around themselves and grow backward ("kinked nanowires"); GaP → InP, GaP → Si, GaAs → InAs, and AlAs → InAs show this behavior (Figure 1c−f). It should be noted that even kinked wires tended to be epitaxial. In general, we do not observe a mixture of straight and kinked morphologies except for a special case discussed below. That is, at least 80% of nanowires exhibited straight or kinked morphology (often approaching 100%) for a given material combination for all growth conditions.

The observed morphologies for each material combination are summarized in Table 1. Here the term "material A" is used for the lower part of the wire, and "material B" for the upper part of the wire. And as above, we use the terms "straight" to refer to wires that continue in the same crystallographic direction after changing material, and "kinked" for wires that tend to change direction or wrap around and grow backward. It is quite striking that, for almost all of the material combinations studied, wires grow straight at one interface (for example, InP → GaP) but kink in the other interface direction (GaP → InP). The only exceptions to this trend were GaP−GaAs, which grew straight in both directions for all growth conditions examined here, and InAs−InP, which is described below. It is important to note also that in no system were kinked wires observed for both

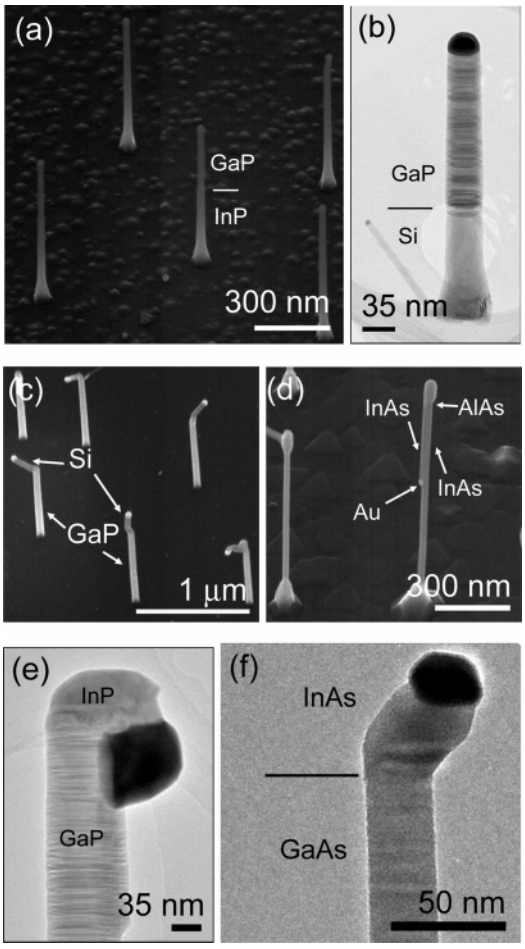

Figure 1. Axial heterostructure nanowire morphology. The scanning electron microscopy (SEM) images are viewed at an angle of 45° to the surface normal. (a) SEM image of InP → GaP nanowires. The change from InP to GaP is accompanied by a slight change in diameter and image contrast. The interface is indicated by a line. (b) Transmission electron microscopy (TEM) image of a Si → GaP nanowire. The Si section is single-crystalline, while the GaP section exhibits stacking faults perpendicular to the growth direction (horizontal lines across the wire). The interface is indicated by a line. (c) SEM image of GaP → Si nanowires. The two materials can be distinguished by their image contrast. In each wire, the Si segment kinks with respect to the GaP when it begins growing. (d) SEM image of InAs → AlAs → InAs nanowires. The first InAs segment was grown for 3 min, following which an AlAs segment was grown for 30 s. This wire section grows straight. The third segment, InAs again, was grown for 2 min. This section wraps around the top of the wire and then grows backward antiparallel to the original growth. (e) TEM image of a GaP → InP nanowire. The InP wraps along the top of the GaP and grows backward, similar to the wires in (d). (f) TEM image of a GaAs → InAs nanowire. The interface is indicated by a line. The InAs grows at an angle with respect to the GaAs, resulting in a kinked wire.

interface directions. More examples of images of the heterostructure combinations summarized in Table 1 can be found in the Supporting Information.

To investigate the processes occurring during heterostructure nucleation, we examined the earliest stages of heterostructure growth in situ using the GaP → Ge system. When growing Ge on pregrown GaP nanowires, nucleation is observed as a small three-dimensional Ge crystal precipitating at the three-phase boundary between the particle (in this case,

Table 1. Lattice Constants, Lattice Mismatch, and Heterostructure Nanowire Morphology for 13 Material Combinations

material A	material B	material A lattice constant (Å)	material B lattice constant (Å)	morphology: B on A[a]	morphology: A on B	mismatch[b] (%)
AlAs	GaAs	5.6605	5.6533	kinked	straight	−0.13
AlAs	GaP	5.6605	5.4512	kinked	straight	−3.70
AlAs	InAs	5.6605	6.0584	kinked	straight	7.03
AlAs	InP	5.6605	5.8686	kinked	straight	3.68
GaAs	GaP	5.6533	5.4512	straight	straight	−3.57
GaAs	InAs	5.6533	6.0584	kinked	straight	7.17
GaAs	InP	5.6533	5.8686	kinked	straight	3.81
GaAs	Si	5.6533	5.4310	kinked	straight	−3.93
GaP	InAs	5.4512	6.0584	kinked	straight	11.14
GaP	InP	5.4512	5.8686	kinked	straight	7.66
GaP	Ge	5.4512	5.6461	kinked		3.58
GaP	Si	5.4512	5.4310	kinked	straight	−0.37
InAs	InP	6.0584	5.8686	straight	kinked/straight[c]	−3.13

[a] Note that "straight" refers to continuation of growth in the same crystallographic direction, while "kinked" refers to a change of growth direction. [b] Mismatch is calculated with respect to material A, according to the formula mismatch $= (a_B - a_A)/a_A$. Therefore, a positive value of mismatch indicates that the lattice constant of material B is larger than that of material A. [c] The morphology type for InAs grown on InP depends on the growth conditions. See text for details.

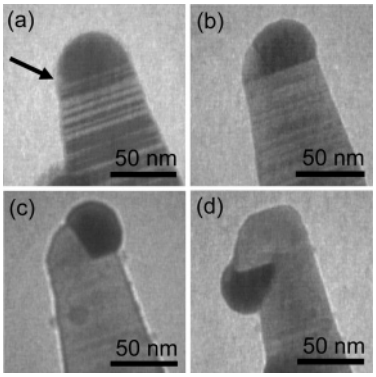

Figure 2. Bright field TEM images recorded during the growth of Ge on GaP nanowires (GaP → Ge interface) by UHV−CVD. Note that these images represent different wires. (a) After the Au particle becomes saturated with Ge, nucleation is observed as a small compact Ge crystal at the boundary between GaP, Au, and the vacuum. This brighter nucleus is indicated by an arrow. The horizontal lines perpendicular to the GaP nanowire are stacking faults. (b) As the nucleus enlarges, the Au particle is pushed horizontally across the GaP surface. Ge does not form a layer on the GaP. (c) As the growth proceeds, a new growth front is visible between the Ge and Au, apparently a different (111) interface. (d) When the particle reaches the edge of the GaP, the growth may continue outward from the wire or may wrap around the top, as shown here. This morphology is very similar to that observed in Figure 1e.

a Au−Ge alloy), GaP wire, and surrounding vacuum (Figure 2a). This nucleus enlarges as more Ge is supplied, and it pushes the particle along perpendicular to the original wire (Figure 2b,c). When the growth interface reaches the edge of the wire, it may bend downward to follow the GaP wire and form an antiparallel segment (Figure 2d), or growth may continue at an angle to or even parallel to the original wire, depending on the details of the particle and nucleus configuration. The result will be a kinked or backward-grown wire, as in Figure 1c, e, or f. The influence of gravity is of course negligible for nanostructures; we see that wire kinking is a consequence of the initial formation of a compact nucleus and its effect on the position of the particle.

When growing one material epitaxially on another, the interface energies between the two materials and the surrounding medium must be considered to understand the resulting morphology.[19] For layer growth to occur, the chemical potential for adsorption of the new material on the substrate must be negative; from this it follows that the Gibbs free energy per unit area G of adsorbed layer must decrease with the number of adsorbed atoms (n) per unit area. For $n = 0$, $G(n)$ is the free energy of the bare substrate, or in other words, the interfacial energy between the substrate and surrounding medium, σ_A. $G(n)$ will tend asymptotically toward the free energy of the bulk adsorbate, α, which at large n is equal to the interface energy between the adsorbate and medium, σ_B. The $n = 0$ intercept of the asymptote is equal to the sum of the two new interface energies, adsorbate−medium and adsorbate−substrate:

$$\alpha_\infty = \sigma_B + \sigma_i \quad (1)$$

Therefore, the difference $\Delta\sigma$ between the sum of the adsorbate−medium and adsorbate−substrate interface energies, and the bare substrate−medium interface energy, must be negative to obtain layer growth:[20]

$$\Delta\sigma = \sigma_B + \sigma_i - \sigma_A < 0 \quad (2)$$

If, however, the difference is positive ($\Delta\sigma > 0$), then the Gibbs free energy per unit area of a uniform adsorbed layer will increase as the number of atoms per unit area increases (toward the bulk adsorbate free energy). In other words, the chemical potential will increase as the number of adsorbed atoms per unit area of substrate increases; thus island growth, rather than layer growth, will be favorable. These two growth modes are referred to as Frank−van der Merwe and

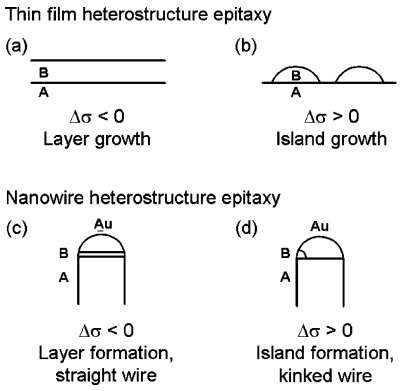

Figure 3. Schematic illustration of a model for nanowire heterostructure nucleation. The energy balance $\Delta\sigma = \sigma_B + \sigma_i - \sigma_A$ determines the mode of growth, where σ_B is the interface energy between the first material (A) and the surrounding medium/Au particle, σ_i is the interface energy between the second material (B) and the first (A), and σ_A is the interface energy between material A and the surrounding medium/Au particle. For thin film growth, (a) $\Delta\sigma < 0$ results in layer-by-layer heteroepitaxial growth; (b) $\Delta\sigma > 0$ results in island growth of B on A. For nanowire heterostructure growth; (c) $\Delta\sigma < 0$ results in the formation of layers and straight nanowire growth; (d) $\Delta\sigma > 0$ results in the formation of islands and kinked nanowire growth.

Volmer−Weber.[21] For any given material combination, we should expect layer growth in one direction and island growth in the other.

We can draw an analogy to this analysis for Au-assisted nanowire growth. First note that, because the growth conditions are chosen to limit conformal growth on the side facets, we can neglect the interface between the semiconductor and surrounding medium. We also neglect any changes in the interface between the alloy particle and the surrounding medium. Then, as above, for a second material (material B) to grow as a layer on a first material (A), the sum of the two new interface energies (Au−B and A−B) must be lower than the A−Au interface energy. If this is not the case, nucleation of material B as an island will be favorable. It is clear then that, for any given material combination, it should be easier to form layers, and thus straight wires, in one direction than in the other. This is illustrated in Figure 3. Incidentally, the trends observed for bulk heteroepitaxial growth (as illustrated in Figure 3a,b) also apply to the conformal growth that occurs on the nanowire side facets during axial heterostructure growth. For the materials combinations we have examined in detail by high-resolution microscopy, in one direction, the conformal growth tends be a flat layer (potentially allowing shell growth), while in the other direction, it is islanded. Because conformal growth was not the focus of the present study, conditions were chosen to suppress it where possible, and it will not be discussed further.

It is important to note that it is not the lattice mismatch, but rather the relevant surface/interface energies, that determine the morphology of axial heterostructure nanowires (although interface energies may of course be indirectly related to lattice mismatch). It is clear from Table 1 that some interfaces with very large lattice mismatch, such as InAs → GaP (11%), grow straight, while the lattice-matched interfaces GaP → Si and AlAs → GaAs do not. In each of these cases, one interface will form layers (and thus straight wires), while the opposite one will exhibit island nucleation. In general, InAs, Si, and Ge always kink when grown on the other materials (these three materials were not grown on each other), InP kinks on all materials except InAs, GaP and GaAs kink on all materials except AlAs (and each other), and AlAs grows straight on all materials.

We did not observe a dependence of heterostructure morphology on the growth conditions used here except for the InAs−InP system. Here, the growth of InP on InAs was always straight. However, when growing InAs on InP, kinked wires were observed at temperatures between 440 and 480 °C when the molar fraction of TMI was at least 6×10^{-6}. Some kinked wires were also observed at the highest temperature investigated (480 °C) with TMI molar fraction 3×10^{-6}. In both of these cases, a mixture of kinked and straight wires was observed. At lower temperatures (380−430 °C) and lower TMI pressures, very few kinked wires were observed. In other words, straight wires containing both heterostructure interfaces (InAs → InP and InP → InAs) could be grown when the temperature and TMI pressure were not too high. Low TMI pressures are optimum for nanowire growth anyway because tapering increases with TMI flow.[14]

It is instructive to consider the two special cases GaAs−GaP and InAs−InP. In each case, straight interfaces are possible for both interface directions although the lattice mismatch is moderate (3.1−3.7%). It may be inferred that, in these cases, the relevant surface energies are similar. This is not surprising because the interactions of Au with GaAs and GaP tend to be similar (in terms of thermodynamics as well as reaction kinetics), as do the interactions of Au with InAs and InP.[15,22,23] As well, it is known that the particle composition changes when the growth material changes. Au can absorb significant amounts of Si and Ge (and indeed, must do so for nanowire growth to be possible) and is also known to absorb large amounts of the group III materials Al, Ga, and In (depending on growth conditions).[15] However, the solubility of the group V materials P and As in Au is negligible under these conditions. This may explain why a change of the group V material has only a small effect on the relevant interface energies, so that the group V component is not correlated with morphology (see Table 1), while changing the group III element has a significant effect on morphology.

The model described here does not account for lattice mismatch in any way. However, when growing planar layers, lattice mismatch cannot be ignored, and consequently, there exists a third possible growth mode, the Stranski−Krastanov mode.[24] In this case, layer growth occurs at first, but strain builds up, and after a few layers, islands form to relieve this strain. The analogous situation in wires would likely result in kinked wires after the formation of a certain number of atomic layers (depending on the materials parameters), with the potential for straight wires when growing a thin enough mismatched interlayer. However, this would mean that wires of certain material combinations would tend to kink in *both*

directions: in one direction immediately due to island formation, and in the other after forming a few layers. Because this was not observed in any system, we conclude that the narrow diameter allows for efficient reduction of interface strain by local diameter modulation.[25] Interestingly, this suggests that there may be a diameter dependence to heterostructure morphology; for nanowire diameters larger than a certain critical diameter, islands may form due to strain, and wire kinking may increase. It should be emphasized that any diameter dependence of the morphology is not considered in this study.

The model described here is purely thermodynamic and does not account for kinetic effects. If the interface energies are similar, then kinetic or other effects may allow us to achieve straight nanowires in both interface directions (as may be happening for InAs−InP). But even if the interface energies are different, presumably other factors can influence the wire morphology. For example, changes in particle composition should affect the interface energies and thus could potentially be used to tune heterostructure growth. The particle composition is expected to depend on temperature, pressure, and materials present, and hence appropriate choice of growth conditions may permit a desirable wire morphology. Residual background material that lingers in the growth system may also play a role: for example, In is known to exhibit a memory effect in MOVPE systems long after it has been used for growth, and we have observed it to be present in the particle after growth of GaP and GaAs nanowires even though it is not present in the wires themselves. Finally, the introduction of small amounts of other materials, analogous to surfactants for layer growth,[26] may change the interface energies in such a way that the nucleation type is affected.

To summarize, although more complex effects may be present, a simple model for axial heterostructure nanowire growth, based on the relationship between the nucleus type and the final wire morphology, can explain straight vs kinked wires having different interface directions. This understanding of nanowire heterostructure formation can also be applied to branched nanostructures (nanotrees) composed of multiple materials. Normally, when growing homogeneous nanotree structures, branches grow outward from the "trunk" (substrate nanowire) in preferential crystal directions (typically ⟨111⟩B for zinc blende structures, ⟨−1120⟩ for wurtzite structures).[28] However, we have previously noted that InP branches grown on GaP nanowires do not grow outward as expected, but crawl along the surface of the nanowires.[27] Figure 4 shows that this behavior is quite understandable given the knowledge that the GaP → InP interface kinks.

If InP forms compact nuclei on the side facets of GaP nanowires, similar to the growth of InP at the tips of GaP wires, then the Au particle would be pushed along by the growing InP branch, staying in contact with the surface (see Figures 4b and 5a). As expected, InP nanowires that form directly on the GaP substrate also crawl. By contrast, GaP branches grown on InP nanowires tend to lift off and form "normal" nanowire branches (as do GaP nanowires that grow directly on the InP substrate) (see Figures 4d and 5b).

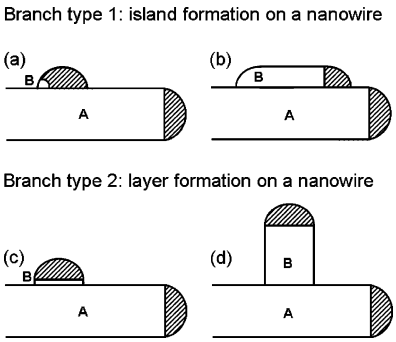

Figure 4. Schematic illustration of the effect of nucleus type on heterostructure branch morphology. (a) Islands may form on the side facets of the trunk nanowire for certain interface energy combinations. (b) After some time, this results in a crawling branch on the side facet. (c) Layers will form on the trunk for other interface energy combinations. (d) The formation of layers leads to straight branch growth.

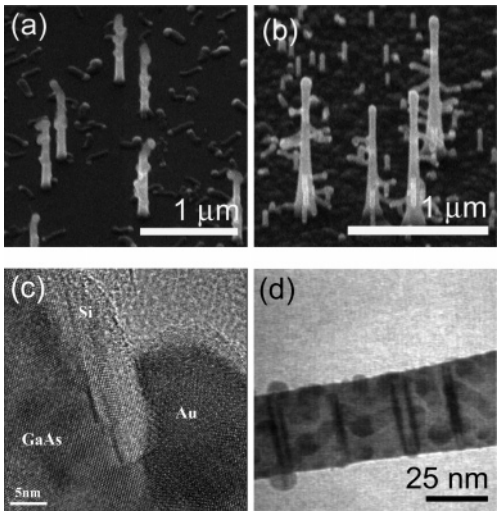

Figure 5. Heterostructure nanotrees with trunks and branches of differing materials. The SEM images are viewed from an angle of 45° to the surface normal. (a) SEM image of crawling InP branches grown on GaP trunks. Previous investigation[27] has shown that these "crawling" branches grow epitaxially on the GaP surface. Note, as well, the crawling InP wires on the substrate. (b) SEM image of GaP branches growing outward from InP trunks. GaP wires on the substrate also grow upward (perpendicular to, and thus epitaxially from, the substrate). (c) High-resolution TEM image of a Si branch grown on a GaAs trunk. The Si branch grows along the surface of the GaAs rather than lifting off; the epitaxial relationship between the two materials can however be confirmed. (d) Bright field TEM image obtained during growth of Ge branches on a GaP trunk (the dark lines are twins in the GaP). The particles are pushed along the surface as the Ge branches grow.

Crawling branch morphology is observed for Si branches growing on GaAs (Figure 5c), again consistent with the island nucleation of Si on GaAs nanowires. As with the formation of axial heterostructures, note that mismatch alone cannot explain the nucleation mode and growth of branches (for example, GaAs → Si has the opposite mismatch to GaP → InP and GaP → Ge).

In situ observations of Ge nanowire branches grown from Au particles on GaP nanowires confirm that nucleation takes the form of a compact island at the edges of the particles and that the nucleus enlarges and pushes the particle around

as it grows, forming crawling wires (see Figure 5d). However, an advantage of in situ observation is the ability to tune growth parameters during growth and to observe the effects. In this way, it was possible to obtain conditions where a majority of Ge nanowire branches lifted off from GaP nanowire trunks. This was primarily achieved by lowering the temperature to the minimum at which growth still occurred while simultaneously maintaining a relatively low Ge pressure. As well, larger particles seemed less likely to result in crawling nanowires. Varying the growth conditions in such a way may, for example, coat the trunk with a conformal Ge layer or change the composition of the particle and thus appropriate interface energies. This result suggests that it may be possible kinetically to achieve good-quality nanowire heterostructures in certain combinations by appropriately tuning growth parameters.

In summary, we have investigated the Au-assisted growth of heterostructure nanowires composed of combinations of GaAs, GaP, InAs, InP, AlAs, Si, and Ge and presented a model to explain the morphology of such heterostructures. This model relates the wire morphology to the nature of the nucleus, either island or layer-type, and, by analogy with planar growth, we suggest that the nucleus type depends on the relationship of the interface energies between the two materials and the particle. This model suggests that, for any combination of two materials, it should be easier to form straight heterostructures in one direction than in the other, and we demonstrate this for the material combinations presented here. The model does not, however, account for kinetics, which may in some cases allow for straight nanowires with two opposite heterostructure interfaces. Additionally, we discuss the possibility of changing interface energies (for example, through the use of surfactants) to allow for straight double heterostructure nanowires. Finally, we demonstrate that branched heterostructure nanotrees follow the same behavior as axial heterostructure nanowires and can be explained by the same model. These results may be useful in the design of complex heterostructure nanowires for advanced applications.

Acknowledgment. Part of this work was performed within the Nanometer Structure Consortium at Lund University and supported by the Swedish Research Council (VR), the Swedish Foundation for Strategic Research (SSF), the Knut and Alice Wallenberg Foundation, and the European Community (EU contract no. 015783 NODE). We acknowledge A. Ellis for his assistance with experimental aspects of the in situ work.

Supporting Information Available: Examples of heterostructure combinations; all images are viewed 45° to the surface normal. This material is available free of charge via the Internet at http://pubs.acs.org.

References

(1) Samuelson, L.; Thelander, C.; Björk, M. T.; Borgström, M.; Deppert, K.; Dick, K. A.; Hansen, A. E., Mårtensson, T.; Panev, N.; Persson, A. I.; Seifert, W.; Sköld, N.; Larsson, M. W.; Wallenberg, L. R. *Physica E* **2004**, *25*, 313.
(2) Li, Y.; Qian, F.; Xiang, J.; Lieber, C. M. *Mater. Today* **2006**, *9*, 18.
(3) Zakharov, N. D.; Werner, P.; Gerth, G.; Schubert, L.; Sokolov, L.; Gösele, U. *J. Cryst. Growth* **2006**, *290*, 6.
(4) Björk, M. T.; Ohlsson, B. J.; Sass, T.; Persson, A. I.; Thelander, C.; Magnusson, M. H.; Deppert, K.; Wallenberg, L. R.; Samuelson, L. *Appl. Phys. Lett.* **2002**, *80*, 1058.
(5) Gudiksen, M. S.; Lauhon, L. J.; Wang, J.; Smith, D. C.; Lieber, C. M. *Nature* **2002**, *415*, 617.
(6) Borgström, M. T.; Verheijen, M. A.; Immink, G.; de Smet, T.; Bakkers, E. P. A. M. *Nanotechnology* **2006**, *17*, 4010.
(7) Svensson, C. P. T.; Seifert, W.; Larsson, M. W.; Wallenberg, L. R.; Stangl, J.; Bauer, G.; Samuelson, L. *Nanotechnology* **2005**, *16*, 936.
(8) Persson, A. I.; Björk, M. T.; Jeppesen, S.; Wagner, J. B.; Wallenberg, L. R.; Samuelson, L. *Nano Lett.* **2006**, *6*, 403.
(9) Regolin, I.; Sudfeld, D., Lüttjohann, S.; Khorenko, V.; Prost, W.; Kästner, J.; Dumpich, G.; Meier, C.; Lorke, A.; Tegude, F.-J. *J. Cryst. Growth* **2007**, *298*, 607.
(10) Magnusson, M. H.; Deppert, K.; Malm, J.-O.; Bovin, J.-O.; Samuelson, L. *Nanostruct. Mater.* **1999**, *12*, 45.
(11) Borgström, M.; Deppert, K.; Samuelson, L.; Seifert, W. *J Cryst. Growth* **2004**, *260*, 18.
(12) Seifert, W.; Borgström, M.; Deppert, K.; Dick, K. A.; Johansson, J.; Larsson, M. W.; Mårtensson, T.; Sköld, N.; Svensson, C. P. T.; Wacaser, B. A.; Wallenberg, L. R.; Samuelson, L. *J. Cryst. Growth* **2004**, *272*, 211.
(13) Dick, K. A.; Deppert, K., Mårtensson, T.; Samuelson, L.; Seifert, W. *J. Cryst. Growth* **2004**, *272*, 131.
(14) Dick, K. A.; Deppert, K.; Samuelson, L.; Seifert, W. *J. Cryst. Growth* **2006**, *297*, 326.
(15) Dick, K. A.; Deppert, K.; Karlsson, L. S.; Wallenberg, L. R.; Samuelson, L.; Seifert, W. *Adv. Funct. Mater.* **2005**, *15*, 1603.
(16) Ross, F. M.; Tersoff, J.; Reuter, M. C. *Phys. Rev. Lett.* **2005**, *95*, 146104.
(17) Hannon, J. B.; Kodambaka, S.; Ross, F. M.; Tromp, R. M. *Nature* **2006**, *440*, 69.
(18) Kodambaka, S.; Tersoff, J.; Reuter, M. C.; Ross, F. M. *Science* **2007**, in press.
(19) Mutaftschiev, B. *Phys. Rev. B* **1989**, *40*, 779
(20) Peierls, R. *Phys. Rev. B* **1978**, *18*, 2013.
(21) Markov, I. V. *Crystal Growth for Beginners: Fundamentals of Nucleation, Crystal Growth, and Epitaxy*; World Scientific Press: Singapore, 1995.
(22) Weizer, V. G.; Fatemi, N. S. *J. Appl. Phys.* **1991**, *69*, 8253.
(23) Hiraki, A.; Shuto, K.; Kim, S.; Kammura, W.; Iwami, M. *Appl. Phys. Lett.* **1977**, *31*, 611.
(24) Seifert, W.; Carlsson, N.; Miller, M.; Pistol, M.-E.; Samuelson, L.; Wallenberg, L. R. *Prog. Cryst. Growth Charact. Mater.* **1996**, *33*, 423.
(25) Larsson, M. W.; Wagner, J. B.; Wallin, M.; Håkansson, P.; Fröberg, L. E.; Samuelson, L.; Wallenberg, L. R. *Nanotechnology* **2007**, *18*, 015504.
(26) Wadley, H. N. G.; Zhou, X.; Johnson, R. A.; Neurock, M. *Prog. Mater. Sci.* **2001**, *46*, 329.
(27) Karlsson, L. S.; Larsson, M. W.; Malm, J. -O.; Wallenberg, L. R.; Dick, K. A.; Deppert, K.; Seifert, W.; Samuelson, L. *NANO* **2006**, *1*, 139.
(28) Dick, K. A.; Deppert, K.; Karlsson, L. S.; Larsson, M. W.; Seifert, W.; Wallenberg, L. R.; Samuelson, L. *MRS Bull.* **2007**, *32*, 127.

NL0705900